Int. Journ. of Laser Science, Vol. 1, pp. 53–71
Reprints available directly from the publisher.
Photocopying permitted by license only.

A Universal Theoretical Model for Thermal Accumulation in Materials During Repetitive Pulsed Laser Processing

C.H. Li[1,2], X. Ju[1,*], W.D. Wu[2], Q.H. Zhu[2] and W.G. Zheng[2]

[1]*University of Science and Technology Beijing, Beijing 100083, China*
[2]*Research Centre of Laser Fusion, China Academy of Engineering Physics, Mianyang 621900, Sichuan Province, China*

This work is designed to present a universal theoretical model to study the repetitive pulsed laser-induced thermal integration process in materials. Thermal integration in materials induced by laser pulses has become a very important issue as a result of that pulsed laser heating is widely employed in high-tech industries such as surface processing, thin solid films, laser machining and three-dimensional (3-D) printing in recent years. In these laser-based techniques, knowledge of the temperature distribution in materials is the basis for optimization of process parameters and product quality control. In this work, using the Green function method, the analytical solution formula for temperature field in materials induced by repetitive pulsed laser heating is mathematically deduced based on the Fourier heat transfer theory. In order to get an analytical solution independent of material properties, the obtained temperature field formula is then derived into the dimensionless form. To investigate the effect of two key parameters of laser pulse on thermal integration process, the pulse spacing to pulse width (t_c/t_h) ratio and the laser intensity ratio are carefully examined with the dimensionless analytical solution formula. Results reveal that both t_c/t_h ratio and laser intensity ratio exert direct influence on the thermal integration process. For a setting value of laser intensity ratio, the thermal integration is mainly controlled by the t_c/t_h ratio, and the peak temperature difference drops exponentially as the t_c/t_h ratio (<25) increase linearly. For a given cooling period, the correlation between peak temperature difference and laser intensity ratio is linearly, and there is a specific laser intensity ratio which in turn results in a steady temperature distribution. Furthermore, the analytical formula is applied to study temperature distribution in materials of SiGe thin solid films and fused silica substrates induced by pulsed laser. The analytical

*Corresponding author: Tel: +86 (0)10 6233 3921; E-mail: jux@ustb.edu.cn

formula of temperature field can be beneficial to thermal integration in materials induced by pulsed laser for lots of laser-based technologies.

Keywords: Laser processing, thermal conduction, thermal integration, analytical formula, pulse parameter, Green function

1 INTRODUCTION

Thermal integration in materials induced by pulsed laser has become a very important question since the high repetition frequency laser has been widely used in modern high-tech industries [1-3]. For instance, pulsed laser is widely employed in field of laser-supported cutting, welding, drilling and surface processing technologies [4-8]. Besides, pulsed laser also find new applications in field of thin solid film deposition techniques [9-11], the three-dimensional (3-D) printing technology [12-13] and the antique surface cleaning processes [14].

Laser-material interaction process involves many complex physical phenomena [15-19], such as photon energy absorption, thermal diffusion and integration, material melting and cooling. For nanosecond laser irradiation, the thermal effects play a crucial role in leading to the heating of materials and the eventually melting and cooling process [20]. Pulsed laser-induced thermal integration in target materials is the basis for these applications since the laser-based material processing depends on it. Thermal integration also is a restriction factor for some situations since it will cause damage in materials. Therefore, the thermal integration in materials during pulsed laser irradiation has aroused increasing interest in recent years [21-23].

In the case of pulsed laser, the integration process consists of successive heating and cooling cycles. The thermal integration mainly depends on the pulse shape, pulse repetition rate and laser intensity. Mendham*, et al.* have studied the influence of variation of temporal pulse shape on laser heating in clusters [22]. The results suggested that the temporal profile of the laser pulse played a crucial role in the laser-induced heating. Kalyon and Yilbas [24] have investigated the effect of variation of pulse parameter on the closed form solution of repetitive laser pulse heating process. They found that the maximum surface temperature increases rapidly once the cooling period between the consecutive pulses is reduced.

Mathematically, the heating process can be expressed by the Fourier heat conduction differential equation with the boundary and initial conditions [25-29]. The resolution of this partial differential equation is normally carried out by numerical methods, such as finite differences and finite elements methods [30-32]; however, numerical methods can not reveal the physical meaning and relations between laser parameters and the heating process. Analytical approaches provide a way to solve this problem. The Green function method is quite attractive because it is an analytical solution which leads to the temperature field without losing the physical aspects involved in the heating process.

In the present study the Green function method is used to analytically solve the Fourier thermal conduction equation which describes the temporal thermal integration in materials induced by repetitive laser pulses at nanosecond pulse. Successive heating and cooling cycles are considered in the analysis. Non-dimensionalized formula was used to analyse the effects of variation of the ratio of pulse spacing to pulse width (repetitive frequency) and the ratio of laser intensity on the thermal integration process. The derived formula is then applied to study temperature distribution in SiGe thin solid film and fused silica glass induced by pulsed laser. We attempt to clarify the relationship between laser pulse parameters and thermal integration process. We present an analytical formula for studying temperature field in materials induced by laser pulses.

2 MODELLING OF PULSED LASER HEATING

2.1 Thermal model description

A fraction of the incident laser energy is absorbed by the irradiated material, and the deposited energy leads to the formation of temperature field.

The physical assumptions for the model are listed as follows:

(i) The model only considers the quasi-steady heat conduction problem. The initial thermal history of the irradiated material is neglected, as can be seen in a number of previous analytical models [33-34];
(ii) The target material is taken as a semi-infinite body and the surface of the material is adiabatic. This assumption results from the fact that the laser beam size is very small relative to the material and the heat losses by convection and radiation are negligible compared to heat conduction within the material during the time of laser irradiation;
(iii) The properties of the irradiated material, such as thermal conductivity, thermal diffusivity and reflectivity, are isotropic and independent of temperature; and
(iv) Phase change of the target material is not considered in this paper.

2.2 Analytical formulation

For mathematical formulation a Cartesian geometry system is employed; the x-y plane of the coordinate system lies on the surface of the target materials and the origin coincides with the centre of the laser beam.

In general form the heat conduction differential equation for one laser heating pulse can be written as

$$\partial^2 T\left(\vec{r},t\right)\Big/\partial\vec{r}^{\,2} + g\left(\vec{r},t\right)\Big/k = \left(1/\alpha\right)\times\partial T\left(\vec{r},t\right)\Big/\partial t \qquad (1)$$
$$0<\vec{r}<\infty, t>0$$

with the boundary conditions:

$$-k\times\partial T\left(\vec{r},t\right)\Big/\partial z = 0,\ z=0,\ t>0 \qquad (2)$$

and

$$\partial T\left(\vec{r},t\right)\Big/\partial z = 0, z=\infty, t>0 \qquad (3)$$

with the initial condition

$$T(\vec{r},0) = T_0, t=0 \qquad (4)$$

where t is time, the thermal conductivity, k, the thermal diffusivity, $\alpha = k/\rho c$, the density, ρ, the specific heat, c, the heat source in the solid, $g\left(\vec{r},t\right)$, and the initial temperature, T_0, are independent of temperature, T.

The surface heating source can be formally expressed as

$$g\left(x,y,z,t\right) = A\times\left(1-r_f\right)\times I_0\times Exp\left[-\frac{x^2}{R_x^2}-\frac{y^2}{R_y^2}\right]\times f\left(t\right) \qquad (5)$$

where A is the material absorptivity, r_f is the reflectivity, I_0 is the peak laser intensity, R_x is the beam radius in the x-direction, R_y is the beam radius in the y-direction and $f(t)$ is the temporal variation of the laser pulse.

Mathematically, the solution of the linear system, in terms of the Green function, is given by

$$T\left(\vec{r},t\right) = T_0 + \frac{\alpha}{k}\int_{-\infty}^{\infty} d\vec{r}\int_{\tau=0}^{t} g\left(\vec{r},t\right)\times G\left(\vec{r},t;\vec{r}',\tau\right)d\tau \qquad (6)$$

where τ is pulsed width. The Green function $G\left(\vec{r},t;\vec{r}',\tau\right)$ satisfies

$$\left(k/\alpha\right)\times\partial G\left(\vec{r},t;\vec{r}',\tau\right)\Big/\partial t - k\times\nabla^2 G\left(\vec{r},t;\vec{r}',\tau\right) = \delta\left(\vec{r}-\vec{r}'\right)\delta\left(t-\tau\right) \qquad (7)$$
$$-\infty<\vec{r}<\infty, t>0$$

and

$$G\left(\vec{r},t;\vec{r'},\tau\right)=0,\ as\ \ \vec{r}\rightarrow\pm\infty \tag{8}$$

Therefore, the Green function can be expressed as

$$\begin{aligned}
&G\left(x,y,z,t\right)\\
&=\left\{\frac{2}{\pi^3}\int_{\lambda=0}^{\infty}\exp\left(-\alpha\lambda^2\left(t-\tau\right)\right)\cos\left(\lambda x'\right)\cos\left(\lambda x\right)d\lambda\right.\\
&\times\int_{\beta=0}^{\infty}\exp\left(-\alpha\beta^2\left(t-\tau\right)\right)\cos\left(\beta y'\right)\cos\left(\beta y\right)d\beta\\
&\left.\times\int_{\mu=0}^{\infty}\exp\left(-\alpha\mu^2\left(t-\tau\right)\right)\cos\left(\mu z'\right)\cos\left(\mu z\right)d\mu\right\}
\end{aligned} \tag{9}$$

where λ is laser beam wavelength; consequently,

$$\begin{aligned}
&\Delta T\left(\vec{r},t\right)=T\left(\vec{r},t\right)-T_0\\
&=\frac{\alpha}{k}\int_{-\infty}^{\infty}d\vec{r}\int_{\tau=0}^{t}g\left(\vec{r},t\right)\times G\left(\vec{r},t;\vec{r'},\tau\right)d\tau\\
&=\frac{\alpha}{k}\int_{-\infty}^{\infty}d\vec{r}\int_{\tau=0}^{t}\frac{A\times\left(1-r_f\right)}{\times I_0\times Exp\left[-\left(x/R_x\right)^2-\left(y/R_y\right)^2\right]\times f\left(\tau\right)}\times G\left(\vec{r},t;\vec{r'},\tau\right)d\tau\\
&=\frac{2\alpha A\left(1-r_f\right)I_0}{k\pi^3}\\
&\quad\times\left\{\int_{-\infty}^{\infty}\exp\left(-x'/R_x^2\right)\cos\left(\lambda x'\right)dx'\int_{-\infty}^{\infty}\begin{matrix}\exp\left(-y'/R_y^2\right)\\ \cos\left(\beta y'\right)dy'\end{matrix}\right\}\\
&\quad\times\int_{0}^{\infty}\exp\left(-\alpha\lambda^2\left(t-\tau\right)\right)\cos\left(\lambda x\right)d\lambda\\
&\quad\times\int_{0}^{\infty}\exp\left(-\alpha\beta^2\left(t-\tau\right)\right)\cos\left(\beta y\right)d\beta\\
&\quad\times\int_{0}^{\infty}\exp\left(-\alpha\mu^2\left(t-\tau\right)\right)\cos\left(\mu z\right)d\mu\int_{\tau=0}^{t}f\left(\tau\right)d\tau
\end{aligned} \tag{10}$$

After a series of integral operation, we obtain the temperature field formula as

$$\Delta T\left(\vec{r},t\right)=\frac{A\left(1-r_f\right)I_0R_xR_y}{k}\sqrt{\frac{\alpha}{\pi}}\times$$

$$\int_{\tau=0}^{t}\frac{Exp\left[-x^2/\left(\begin{matrix}4\alpha\\(t-\tau)\end{matrix}\right)+R_x^2\right]Exp\left[-y^2/\left(\begin{matrix}4\alpha\\(t-\tau)\end{matrix}\right)+R_y^2\right]Exp\left[\begin{matrix}-z^2/4\alpha\\(t-\tau)\end{matrix}\right]}{\sqrt{t-\tau}\sqrt{4\alpha\left(t-\tau\right)+R_x^2}\sqrt{4\alpha\left(t-\tau\right)+R_y^2}}f\left(\tau\right)d\tau \tag{11}$$

And, for the case of a circular shape beam with radius of, R:

$$R_x=R_y=R \tag{12}$$

so

$$\Delta T\left(x,y,z,t\right)=\frac{A\left(1-r_f\right)I_0R^2}{k}$$
$$\sqrt{\frac{\alpha}{\pi}}\int_{\tau=0}^{t}\frac{Exp\left[-\frac{x^2+y^2}{4\alpha\left(t-\tau\right)+R^2}\right]Exp\left[-\frac{z^2}{4\alpha\left(t-\tau\right)}\right]}{\sqrt{t-\tau}\times\left(4\alpha\left(t-\tau\right)+R^2\right)}f\left(\tau\right)d\tau \tag{13}$$

2.3 Non-dimensionalizing and repetitive pulse properties

In order to generalize the analytical solution independent of specific material properties and laser intensity, which can be applicable to any material, non-dimensionalizing of the parameters is essential.

As introducing the following parameters:

$$t^*=\frac{\alpha\left(t-\tau\right)}{R^2},\ x^*=\frac{x}{R},\ y^*=\frac{y}{R},$$
$$z^*=\frac{z}{R},\ T^*=T\frac{k}{I_0\left(1-r_f\right)R}\frac{\sqrt{\pi}}{A} \tag{14}$$

Substituted this time function into the integral we can get the non-dimensionalized formulae for calculation:

$$\Delta T^*=\int_{\tau^*-0}^{t^*}\frac{Exp\left[\frac{x^{*2}+y^{*2}}{1+4(t^*-\tau^*)}\right]Exp\left[\frac{z^{*2}}{4(t^*-\tau^*)}\right]}{\sqrt{t^*-\tau^*}\left(1+4\left(t^*-\tau^*\right)\right)}f(\tau^*)d\tau^* \tag{15}$$

For the actual laser processing situation, repetitive pulsed laser with successive heating and cooling process and various laser intensity of laser pulse must be considered.

Mathematically, a high-intensity pulse followed by pulses of the same pulse length but different repetition rates and different laser intensities is introduced in our model. In the pulsed laser operation mode, the energy is supplied at regular intervals with cooling periods. The first pulse starts at t_0=0 with a pulse length and the successive pulse initiates at t_2 with a same pulse length. The heating cycle starts with the initiation of the pulse and ends when the laser intensity reduces to zero. The cooling cycle starts after the pulse ends. The mathematical construction of this repetitive heating and cooling processes is achieved by the introduction of the Heaviside function.

The repetitive pulse can, therefore, be expressed as

$$f(t)+1\times\sum_{u-0}^{n}(-1)^{u}H(t-ut_{p}) \tag{16}$$

Substituted this time function into the integral we can obtain

$$\Delta T^{*}=\sum_{u-0}^{n}(-1)^{u}\int_{\tau^{*}-0}^{t^{*}}\frac{Exp\left[\dfrac{x^{*2}+y^{*2}}{1+4(t^{*}-\tau^{*})}\right]Exp\left[\dfrac{z^{*2}}{4(t^{*}-\tau^{*})}\right]}{\sqrt{t^{*}-\tau^{*}}\left(1+4\left(t^{*}-\tau^{*}\right)\right)}H(\tau^{*}-ut_{p})d\tau^{*} \tag{17}$$

The pulse shape properties used in this study are listed in Table 1 and Table 2.

3 ANALYSIS OF THE THEORETICAL RESULTS OF THE NON-DIMENSIONALIZED MODEL

3.1 Effects of pulse spacing to pulse width ratio on temperature distribution

Figure 1 presents the temporal variation of non-dimensional temperature distribution on the surface of the material at the spot centre for various pulse spacing (cooling period, t_c) to pulse width (heating period, t_h) ratios (t_c/t_h) with a constant intensity ratio. As is depicted by Figure 1, the thermal integration process consists of successive heating period and cooling period. The temperature peaks of each heating period are distinctly depended on the ratios of pulse spacing to pulse width. As is shown in Figure 1, the temperature peaks associated with each successive pulse gradually decrease with the prolongation of cooling time. This is evident from Figure 2 in which the peak

TABLE 1
Pulse parameters for a constant intensity ratio with a variable cooling period.

Pulse Duration	Cooling Period	First Pulse Intensity	Laser Intensity Ratio
20	20	1	1.00
20	40	1	1.00
20	60	1	1.00
20	100	1	1.00

TABLE 2
Pulse parameters for a constant cooling period with a variable intensity ratio.

Pulse Duration	Cooling Period	First Pulse Intensity	Laser Intensity Ratio
20	20	1	1.00
20	20	1	0.60
20	20	1	0.40
20	20	1	0.25

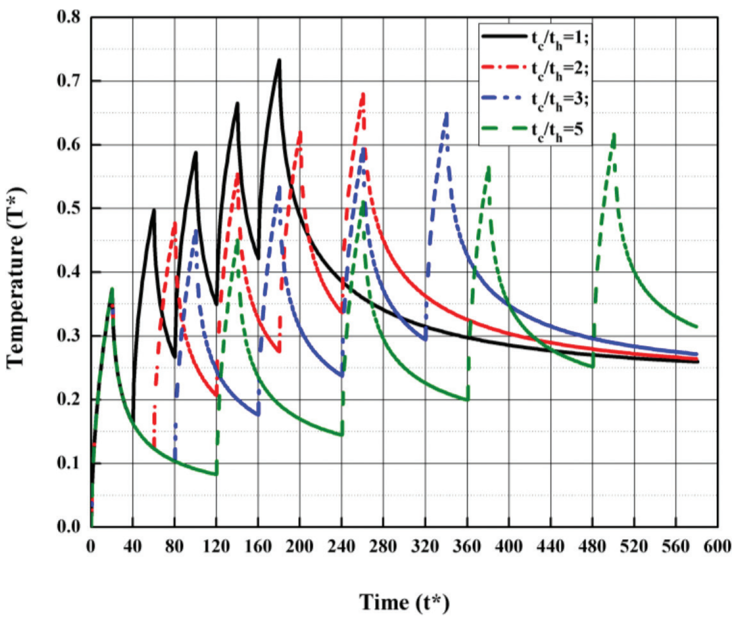

FIGURE 1
Evolution of dimensionless temperature as the function of time for various ratios of pulse spacing to pulse width with a constant intensity ratio.

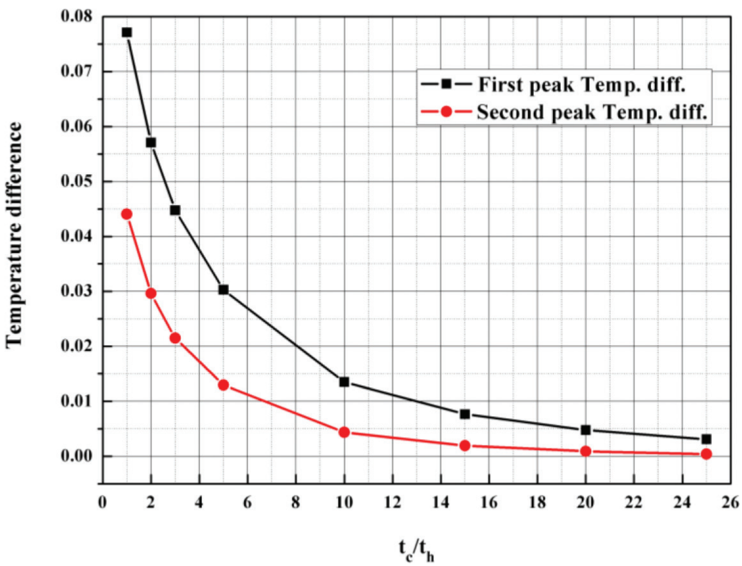

FIGURE 2
Variation of the peak temperature differences as the function of ratios of pulse spacing to pulse width with a constant intensity ratio.

temperature difference *versus* t_c/t_h ratio is shown. It should be noted that the first peak temperature difference is obtained by subtraction of the second peak temperature from the initial peak temperature. Similarly, the second peak temperature difference is obtained by subtraction of the third peak temperature from the second peak temperature. It is apparent that the peak temperature difference decreases exponentially as the t_c/t_h ratio increases linearly.

As is depicted in Figure 1 and Figure 2, on reducing the t_c/t_h ratio smaller than 25, the temperature peaks corresponding to each successive pulse increase further and a higher temperature than the initial peak is attained; therefore, the thermal integration can be controlled by increasing the t_c/t_h ratio even if the intensity of the successive pulses is kept the same as the initial pulse. This situation indicate that if the used laser power was not high enough to induce the peak temperature of target material reach the melting point in the first few pulses, the set t_c/t_h ratio should be smaller than 25, and thus the melting temperature on the target surface will be obtained after several laser pulses due to thermal integration. If the t_c/t_h ratio bigger than 25, the thermal integration process will reached a balanced state. The following peak temperature of successive laser pulse will as the same as the first peak temperature. In this situation, if we make the first peak temperature reach the melting point of the target material by control of the laser intensity or other parameters, we can ensure the temperature on the target surface exactly equal or slightly higher than the melting point just by set the t_c/t_h ratio bigger than

25; therefore, this analytical model should have factual meaning for pulsed laser-based material processing.

For the heating period Figure 1 also shows that the temperature rise rate in the early period is evidently higher than that of the later heating period. This can also be seen from Figure 4, in which time derivative of temperature gradient is shown. The derivative of non-dimensional temperature *versus* time drops sharply in the early period. This suggests that the absorption process of irradiation energy dominates the conduction losses from the surface to the solid in the early period. That is, the energy absorption process by the electrons and successive collisions of excited electrons due to laser-induced photon-electron interaction results in a rapid and substantial temperature increase in the early period. As the heating period progresses, the energy dissipated into the solid bulk through the conduction process becomes significant. This suppresses slightly the rapid temperature rise after the initial heating period. When the cooling cycle starts, energy transfer from the lattice site atoms in the vicinity of the surface to the solid bulk increases. The temperature rises to a value again as the second pulse arrives after the former cooling period; therefore, the ratio t_c/t_h has a direct influence on the thermal integration.

As is depicted by Figure 3, the temperature response to consecutive pulses differs depending on the depths inside the bulk material. Temperature drops sharply as the depth slightly increases, especially in the surface layer region. It is can be explained by the fact that heat conduction through diffusion is

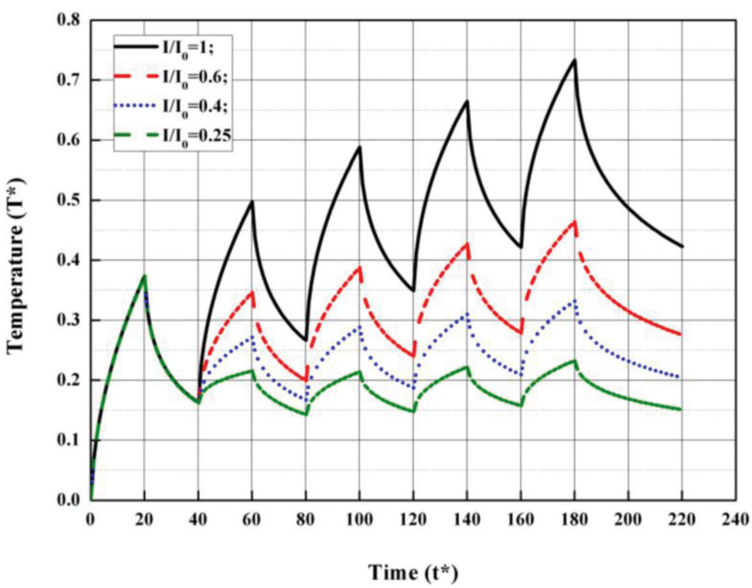

FIGURE 3
Variation of dimensionless temperature at different depth (z-axis) locations as the function of time.

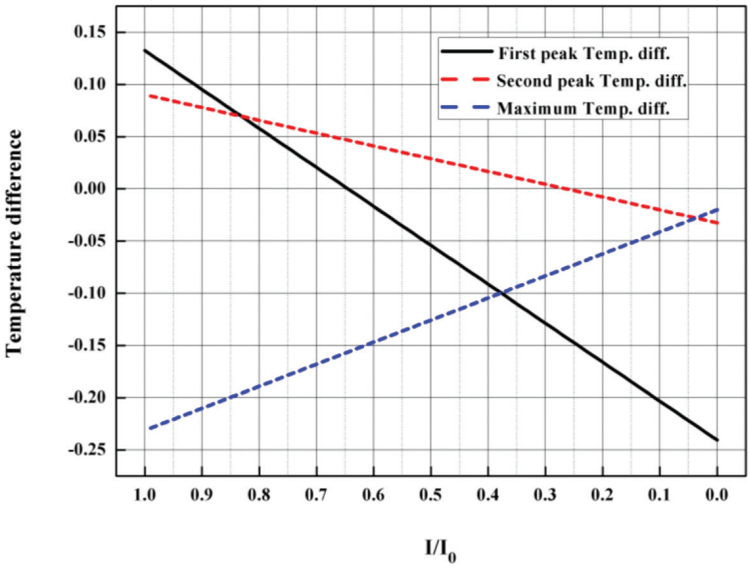

FIGURE 4
Variation of derivative for dimensionless temperature at different depth (z-axis) locations as the function of time.

suppressed by the process of laser energy absorption in the absorption depth region. This situation is depicted more explicitly in Figure 4. Temperature profiles exhibit almost similar in depths bulk that under beneath the absorption depth layer. As the depth increases further, the temperature profile changes and the corresponding derivation profile also varies. This can be explained by considering that the heat conduction mechanism governs the temperature rise in the inside bulk, while the temperature rise due to laser energy absorption can be negligible. Therefore, the temperature gradient reduces and the material response to pulses also slows down.

3.2 Effects of laser intensity ratio of successive pulse on temperature distribution

Figure 5 shows the surface temperature *versus* time for four particular laser intensity ratios referencing to the initial laser intensity with a constant cooling period. Peak temperature corresponding to the successive pulses all exhibits a higher value than the initial peak for the same consecutive pulses (I/I = 1.00); however, at a lower value of laser intensity ratio (I/I = 0,60, 0.40, 0.25), the following peak temperature first decreases during the first couple of successive pulses and then still increases as the heating pulses progress. This is also evident in Figure 6 where the values of first peak temperature difference is obtained by subtraction the first peak temperature from the second peak temperature, and the second peak temperature difference is obtained by

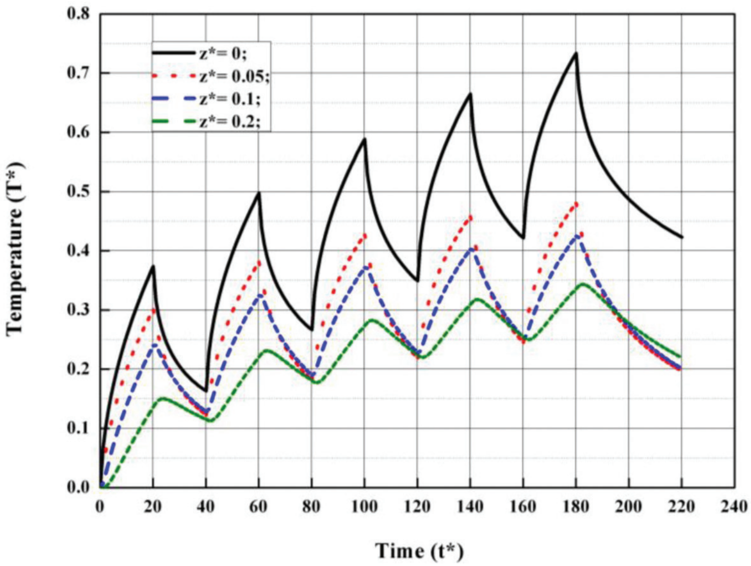

FIGURE 5
Variation of dimensionless temperature on the surface as the function of time for various laser intensity ratios and a constant cooling period.

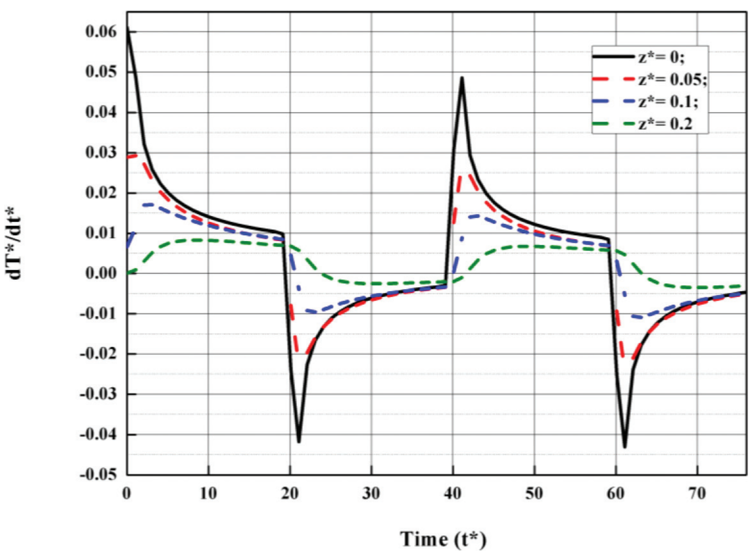

FIGURE 6
Variation of the dimensionless peak temperature difference as the function of laser intensity ratios with a constant cooling period.

subtraction the first peak temperature from the third peak temperature. The maximum temperature difference is obtained by subtraction of the minimum temperature between the second and third pulses from the second peak temperature. It is apparent that the first and second peak temperature difference decreases linearly as the laser intensity ratio decreases from 1.00 to 0.00. As is shown in Figure 6, for a particular cooling period, the maximum temperature difference keeps smaller than zero, which indicates that the following peak temperatures will slightly increase despite the change of laser intensity ratios; therefore, for a given cooling period, there is a specific laser intensity ratio which in turn results in a steady temperature distribution.

4 APPLICATION OF THE MODEL

To illustrate the applicability and usefulness of the presented theoretical deduced equations, the temperature distributions in three typical materials induced by laser pulse have been calculated according to Equations (13) to (15). The pulsed laser-induced epitaxy (PLIE) process has been widely employed in field of thin solid films, semi-conductive devices and quantum cascade lasers for terahertz. For instance, SiGe film for high quality devices consist of a good epitaxy Ge layer with precise thickness deposited on the silicon substrates. The epitaxial SiGe layer is formed by the process of rapid melting of the Ge layer on the Si substrate induced by laser pulse. Laser heating induced target material melting is a key step in the process. In another case, pulsed laser heating also induce damage and breakdown in materials. Because of its excellent optical transmittance and mechanical properties, fused silica glass has been widely used as transmission and diffraction optics in high power laser system. However, high power pulsed laser-induced damage in optics have become a big obstacle in recent years since it's strictly restrict the running of large laser systems. The surface damage is initiated at the laser energy absorption and temperature rising at defects and contaminates in the surface layer, such as platinum metal particles caused by glass fabrication process.

In these situations the temperature distribution in materials induced by pulsed laser is the key information for material processing or protecting. The physical parameters of germanium, platinum and fused silica glass are summarized in Table 3. The used laser wavelength, pulse duration is 1064 nm and 10 ns, respectively. The radius of the focused laser beam on the sample plane is $R = R_x = R_y = 0.564\,\text{mm}$. The laser beam can delivers an energy density between 0 and $40\,\text{J/cm}^2$ on the sample plane. The temperature distribution in the selected materials is calculated based on Equations (13) to (15). Figure 7 and Figure 8 illustrate the temperature evolution on

TABLE 3
Physical parameters of the calculated materials.

Parameters	Ge	Pt	Fused Silica Glass
Melting point (K)	1211.25	2042.00	2000.00
Density (g/cm^3)	5.35	21.50	2.20
Absorptivity	0.445	0.300	2×10^{-6}
Thermal conductivity (W/cmK)	1.5276	0.6688	0.0138
Specific heat (J/gK)	0.3615	0.1296	0.7500

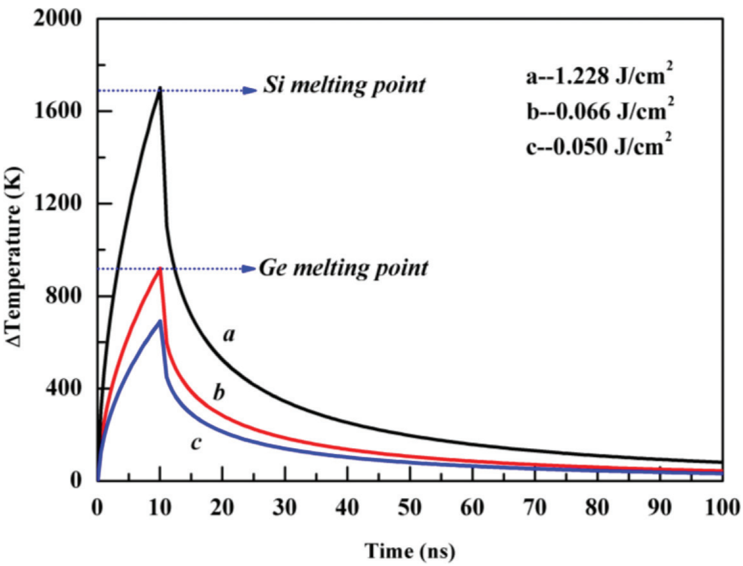

FIGURE 7
Calculated temperature rise (over the ambient temperature) *versus* time on the material surface ($x = y = \ = 0$) for SiGe thin solid film irradiated by a laser beam.

the surface in the spot centre ($x = y = 0$) as the function of time after one pulse laser irradiation. Figure 9 shows the temperature distribution along the depth direction inside the bulk material at the spot centre. Results suggest that a single laser shot at a given fluence of 0.066 J/cm^2 can heat the surface material reach the melting point of germanium. But this fluence laser irradiation is not enough to obtain a SiGe melting layer. If the laser fluence is elevated to 1.228 J/cm^2, the obtained peak temperature (1700 K) is slightly higher than the melting point of the silicon (1683 K) substrate. This temperature is essential for the formation of SiGe alloy since a Ge

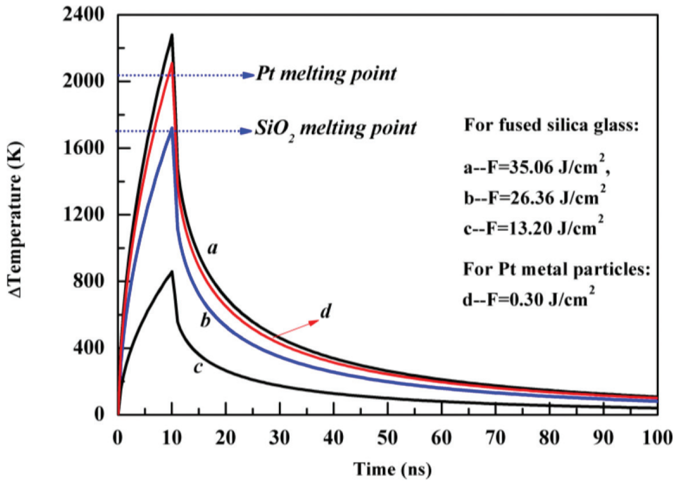

FIGURE 8
Calculated temperature rise (over the ambient temperature) *versus* time on the material surface ($x = y = z = 0$) for SiO_2 glass and Platinum metal irradiated by laser a laser beam.

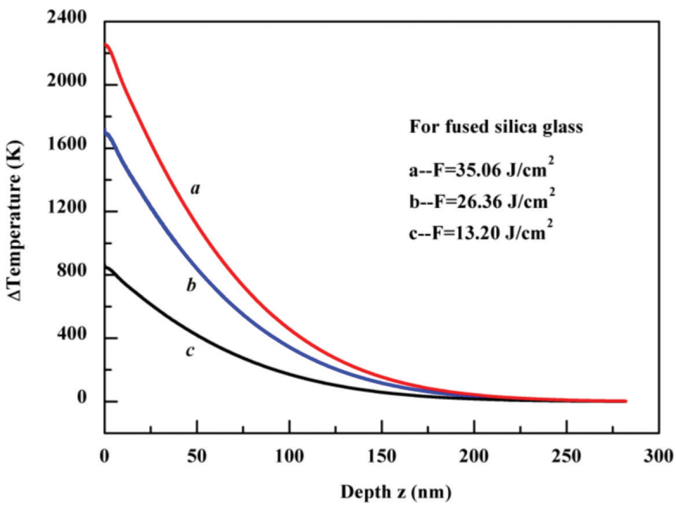

FIGURE 9
Calculated temperature distribution (over the ambient temperature) *versus* depth (z-axis) locations inside the material on the spot centre ($x = y = 0$) for SiO_2 glass irradiated by a laser beam.

layer can be melted. The calculated peak temperature in surface of fused silica can reach the melting point of silica glass (2000 K) as the laser fluence reached 26.360 J/cm^2. But, if there are platinum particles in the surface layer, the local temperature at Pt particles will easily surpass 2000 K even at relatively low laser fluence. This verifies that surface damage in optics mainly depends on defects such as metal particles. Figure 9 gives the temperature distribution along the depth direction inside the bulk material at the spot centre. It is clear that the distribution of temperature rise is locally restricted in the surface layer about 100 nm. The thermal accumulation can be neglected as the cooling time is longer than 25-times of the pulse length (10 ns). These results are in good agreement with experimental works on the formation of SiGe film by PLIE process [35-36] and laser induced damage threshold test of fused silica glass optics [37]. These theoretical calculations can be very beneficial to actual experimental works such as select proper laser parameters for investigating the PLIE process and set safe running fluence for avoiding laser damage in materials.

5 CONCLUSIONS

Using the Green function method, a universal analytical model for temperature field in materials induced by pulsed laser has been successfully presented. This analytical model can be applied to study the spatial and temporal distribution in materials induced by pulsed laser. The presented dimensionless analytical formula for temperature field in materials is used to analyse the effects of variation (cooling period, t_c) to pulse width (heating period, t_h) ratios (t_c/t_h) and laser intensity ratio on temperature distribution in materials. Results reveal that the rate of temperature rise in the early heating period is higher than that in the longer heating periods. In this case, internal energy gain dominates over the conduction energy transfer from surface vicinity to the solid bulk of the substrate material. The material response to consecutive pulses at some depths inside the bulk differs. Temperature decays sharply as the depth slightly increases; however, as the depth further increases larger than a particular depth (the absorption depth), the temperature gradient reduces and the materials response to pulses also slows down. The magnitude of thermal integration is mainly determined by the pulse spacing to pulse width ratios. Peak temperature difference decreases exponentially as the t_c/t_h ratio increases linearly. For a given cooling period there is a specific laser intensity ratio which in turn results in a steady thermal integration process. The theoretical formula is successfully applied to study temperature distribution in SiGe thin solid film and fused silica optics induced by pulsed laser.

ACKNOWLEDGEMENT

The authors acknowledge the financial support by the National Natural Science Foundation of China under Grant No. 51306165.

NOMENCLATURE

A	Material absorptivity
c	Specific heat capacity (J/kgK)
$f(t)$	Temporal variation of the laser pulse
I_0	Peak laser intensity (W)
k	Thermal conductivity (W/mK)
r_f	Reflectivity
R	Laser beam radius (m)
R_x	Laser beam radius in the x-direction (m)
R_y	Laser beam radius in the y-direction (m)
T	Time (seconds)
T	Temperature (K)
T_o	Initial temperature (K)

Greek symbols

α	Thermal diffusivity (m^2/s)
λ	Laser beam wavelength (m)
ρ	Density (kg/m^3)
τ	Laser pulse width (seconds)

REFERENCES

[1] Holtkamp J., Eifel S. and Ryll J. Material processing with ultra-short pulsed lasers: potentials, requirements, approaches. *Laser Technik Journal* **11**(2) (2014), 36–39.

[2] Andre M.L. Status of the LMJ project. *Proceedings of SPIE* **3047** (1996), 38–42.

[3] Lowdermilk W.H. Status of the National Ignition Facility project. *Proceedings of SPIE* **3047** (1996), 16–37.

[4] Atabaki M.M., Nikodinovski M., Chenier P., Ma J., Liu W. and Kovacevic R. Experimental and numerical investigations of hybrid laser arc welding of aluminum alloys in the thick T-joint configuration. *Optics & Laser Technology* **59** (2014), 68–92.

[5] Akbari M.M., Saedodin S., Toghraie D., Shoja-Razavi R. and Kowsari F. Experimental and numerical investigation of temperature distribution and melt pool geometry during pulsed laser welding of Ti6Al4V alloy. *Optics & Laser Technology* **59** (2014), 52–59.

[6] Mackwood A.P. and Crafer R.C. Thermal modelling of laser welding and related processes: a literature review. *Optics & Laser Technology* **37**(2) (2005), 99–115.

[7] Eltawahni H.A., Hagino M., Benyounis K.Y., Inoue T. and Olabi A.G. Effect of CO_2 laser cutting process parameters on edge quality and operating cost of AISI316L. *Optics & Laser Technology* **44**(4) (2012), 1068–1082.

[8] Schuocker D., Aichinger J. and Majer R. Dynamic phenomena in laser cutting and process performance. *Physics Procedia* **39** (2012), 179–185.

[9] Sharma A.K., Ayyub P., Multani M.S., Adhi K.P., Ogale S.B., Sunderaraman M., Upadhyay D.D. and Banerjee S. Synthesis of crystalline carbon nitride thin films by laser processing at a liquid-solid interface. *Applied Physics Letters* **69**(23) (1996), 3489–3491.

[10] Bovatsek J., Tamhankar A., Patel R.S., Bulgakova N.M. and Bonse J. Thin film removal mechanisms in ns-laser processing of photovoltaic materials. *Thin Solid Films* **518**(10) (2010), 2897–2904.

[11] Das M., Balla V.K., Basu D., Manna I., Kumar T.S.S. and Bandyopadhyay A. Laser processing of in situ synthesized TiB-TiN reinforced Ti6Al4V alloy coatings. *Scripta Materialia* **66**(8) (2012), 578–581.

[12] Pereira T.F., Oliveira M.F., Maia I.A., Silva J.V.L., Costa M.F. and Thire R.M. 3-D Printing of poly (3-hydroxybutyrate) porous structures using selective laser Sintering. *Macromolecular Symposia* **319**(1) (2012), 64–73.

[13] Blair J.J. Investigation of Laser Printing for 3D Printing and Additive Manufacturing. PhD thesis, University of Warwick. 2013.

[14] Gan X.J., Chen Y. and Li L. Laser cleaning of neutral attenuator plate based on low power laser diode. *Advanced Materials Research* **614-615** (2012), 1547–1552.

[15] Stuart B.C., Feit M.D., Rubenchik A.M., Shore B.W. and Perry M.D. Laser-induced damage in dielectrics with nanosecond to sub picosecond pulses. *Physical Review Letters* **74**(12) (1995), 2248–2251.

[16] Kubota A., Caturla M.J., Stolken J.S. and Feit M.D. Densification of fused silica due to shock waves and its implications for 351 nm laser induced damage. *Optics Express* **8**(11) (2001), 611–616.

[17] Awazu K. Ablation and compaction of amorphous SiO_2 irradiated with ArF excimer laser. *Journal of Non-Crystalline Solids* **337**(3) (2004), 241–253.

[18] Wong J., Ferriera J.L., Lindsey E.F., Haupt D.L., Hutcheon I.D. and Kinney J.H. Morphology and microstructure in fused silica induced by high fluence ultraviolet 3ω (355 nm) laser pulses. *Journal of Non-Crystalline Solids* **352**(3) (2006), 255–272.

[19] Norton M.A., Hrubesh L.W., Wu Z.L., Donohue E.E., Feit M.D., Kozlowski M.R., Milam D., Neeb K.P., Molander W.A., Rubenchik A.M., Sell W.D. and Wegner P. Growth of laser-initiated damage in fused silica at 351 nm. *Proceedings of SPIE* **4347** (2001), 468–482.

[20] Chichkov B.N., Momma C., Nolte S., Alvensleben F.V. and Tunnermann A. Femtosecond, picosecond and nanosecond laser ablation of solids. *Applied Physics A: Materials Science & Processing* **63**(2) (1996), 109–115.

[21] Yilbas B.S. and Kalyon M. Repetitive laser pulse heating with a convective boundary condition at the surface. *Journal of Physics D: Applied Physics* **34**(2) (2001), 222–231.

[22] Mendham K.J., Tisch J.W.G., Mason M.B., Hay N. and Marangos J.P. Control of laser heating in clusters through variation in temporal pulse shape. *Optics Express* **11**(12) (2003), 1357–1364.

[23] Yilbas B.S. and Sami M. Thermal integration in laser pulse heating-a kinetic-theory approach. *Journal of Physics D: Applied Physics*. **30**(22) (1997), 3088–3095.

[24] Kalyon M. and Yilbas B.S. Repetitive laser pulse heating analysis: Pulse parameter variation effects on closed form solution. *Applied Surface Science* **252**(6) (2006), 2242–2250.

[25] Yang S.T., Matthews M.J., Elhadj S., Draggoo V.G. and Bisson S.E. Thermal transport in laser irradiated fused silica: *In situ* measurements and analysis. *Journal of Applied Physics* **106**(10) (2009), 103106.

[26] Conde J.C., Gonzalez P., Lusquinos F., Chiussi S., Serra J. and Leon B. Analytical and numerical calculations of the temperature distribution in Si and Ge targets irradiated by excimer lasers. *Applied Surface Science* **248**(1-4) (2005), 455–460.

[27] Conde J.C., Lusquinos F., Gonzalez P., Leon B. and Perez-Amor M. Temperature distribution in a material heated by laser radiation: modelling and application. *Vacuum* **64**(3-4) (2002), 359–366.

[28] Shuja S.Z., Yilbas B.S. and Khan S.M.A. Laser heating of semi-infinite solid with consecutive pulses: Influence of material properties on temperature field. *Optics & Laser Technology* **40**(3) (2008), 472–480.

[29] Li J.F., Li L. and Stott F.H. Comparison of volumetric and surface heating sources in the modeling of laser melting of ceramic materials. *International Journal of Heat & Mass Transfer* **47**(6-7) (2004), 1159–1174.

[30] Jendrzejewski R., Sliwinski G., Krawczuk M. and Ostachowicz W. Temperature and stress fields induced during laser cladding. *Computers & Structures* **82**(7-8) (2004), 653–658.

[31] Yun H.J. Numerical simulation of vertical temperature distribution in heterogeneous multilayer structure with Mathematica. *Applied Surface Science* **214**(1-4) (2003), 312–318.

[32] Yilbas B.S., Sami M. and AbuAlHamayel H.I. 3-dimensional modeling of laser repetitive pulse heating: a phase change and a moving heat source considerations. *Applied Surface Science* **134**(1-4) (1998), 159–178.

[33] Araya G. and Gutierrez G. Analytical solution for a transient, three-dimensional temperature distribution due to a moving laser beam. *International Journal of Heat & Mass Transfer* **49**(21-22) (2006), 4124–4131.

[34] Milosevica N. D. and Raynaud M. Analytical solution of transient heat conduction in a two-layer anisotropic cylindrical slab excited superficially by a short laser pulse. *International Journal of Heat & Mass Transfer* **47**(8-9) (2004), 1627–1641.

[35] Berti M., Mazzi G., Calcagnile L., Drigo A.V., Merli P.G. and Migliori A. Composition and structure of Si-Ge layers produced by ion implantation and laser melting. *Journal of Materials Research* **6**(10) (1991), 2120–2126.

[36] Watakabe H., Sameshima T., Kanno H., Sadoh T.and Miyao M. Electrical and structural properties of poly-SiGe film formed by pulsed-laser annealing. *Journal of Applied. Physics* **95**(11) (2004), 6457–6461.

[37] Genin F.Y., Sheehan L.M., Yoshiyama J.M., DiJon J. and Garrec P. Statistical study of UV-laser-induced failure of fused silica. *Proceedings of SPIE* **3244** (1997), 155–163.